Mausam, (1994), 45, 4, 303-314

551.501 : 551.553.21 : 551.515.11 (267.64)

Application of remote sensing in the study of monsoon energetics over Bay of Bengal during summer monsoon

V. K. GOSWAMI and D. N. SIKDAR*
Air Force Academy, Hyderabad-500043 (India)
(Received 22 March 1993, Modified 16 December 1993)

सार — टाइरॉस-एन (टी. आई. आर. ओ. एस.-एन.) उपग्रह से प्राप्त चित्रों के उपयोग से मेघ तथा मानसून अवदाब क्षेत्रों का अध्ययन किया गया और फिर ग्रीष्मकालीन मानसून के दौरान बंगाल की खाड़ी में मानसून ऊर्जा-विज्ञान के अध्ययन का प्रयास किया गया। बंगाल की खाड़ी में कुछ चुनिंदा अवस्थाओं में 27 जून-6 अगस्त 1979 के दौरान 10° × 10° ग्रिड बॉक्स (अर्थात् 15-25° उ० और 85-95° पू०) के अंतर्गत 700 हे. पा. तल पर गतिज लक्षणों अर्थात् सृति (झुकाव), भ्रमिलता और ऊर्ध्वाधर वेगों का अभिकलन किया गया। इसके बाद, अमेरिका के अनुसंधान वायुयान से प्राप्त ड्राप विंड सौंदे आंकड़ों के उपयोग से लैग्रैनजियन फ्रेम में विशिष्ट विक्षुब्ध अवस्था के शुद्धगतिक लक्षणों का अध्ययन किया गया; संबद्ध मानसून अवदाब के विकास संबंधी लक्षणों का पता लगाने के लिए 'यू' और 'वी' आंकड़ों की रूपरेखा बनाई गई।

सचमैन आदि (1977) तथा गोस्वामी आदि (1990) के मेघ गुच्छ अध्ययनों का अनुसरण करते हुए गुच्छ संलयन सिद्धांत (सी. सी. टी.) एवं बृहत् गुच्छ सिद्धांत (जी. सी. टी.) के अनुसार मानसून अवदाब के वास्तविक से लगने वाले दो मॉडल बनाए गए हैं।

गोस (जी. ओ. ई. एस.) उपग्रह के चित्रों के उपयोग से मानसून अवदाब के अंदर और उसके चारों ओर बड़े पैमाने पर ऊर्ध्वाधर परिसंचरण किया गया। शुद्धगतिक अध्ययनों से पता चला कि ऊर्ध्वाधर वेगों, भ्रमिलता और सृति के उच्च मान अधिकतम संयोजी मेघ व्याप्ति जैसे हैं अर्थात् मानसून अवदाब की निर्माण और परिपक्व अवस्थाओं से मेल खाते हैं।

ABSTRACT. An attempt has been made to study the monsoon energetics over Bay of Bengal by studying the cloud and monsoon depression fields during summer monsoon using TIROS-N satellite imageries. The 700 hPa kinetic features, *e.g.*, vergence, vorticity and vertical velocities for a few selected phases in the Bay of Bengal during 27 June-6 August 1979 within the 10° × 10° grid box (*i.e.*, 15-25°N & 85-95°E) were computed. Next, the kinematic features of a typical disturbed phase (5-7 July 1979) were studied in a Lagrangian frame by using drop wind sonde data of U.S. research aircraft. The data profiles *u* and *v* have been drawn to identify the evolutionary features of an associated monsoon depression.

Following Suchman *et al.* (1977) and the cloud cluster studies of Goswami *et al.* (1990); the two plausible models of monsoon depression have been postulated in terms of Cluster Coalescence Theory (CCT) and Giant Cluster Theory (GCT).

The vertical mass circulations within and around the monsoon depression were inferred by making use of GOES imageries. The kinematic studies have revealed that the higher values of vertical velocities, positive verticity and vergence correspond with the maximum connective cloud coverage *vis-a-vis* forming and mature stages of monsoon depression.

Key words — Cloud fields, Monsoon energetics, Kinematic features, Vorticity, Vertical velocity, Cloud cluster models, Cloud coalescence theory, Giant cluster theory.

1. Introduction

The qualitative and quantitative estimation of the precipitation involving time and space variation constitutes an important aspect of long, medium, and short range forecasting on different scales, *viz.*, global, macro, synoptic, meso and micro. Unlike the other weather phenomena the monsoonal precipitation is a widespread phenomenon of quasi-continuous nature, barring a few instances of short-lived temporary precipitation arising due to local genesis. Although, any specific event in any given area is dependent only partially on the local structure of the atmosphere inside the region, the major control comes from the broad scale situations existing over very large areas, specially it is so in the case of summer monsoon. The broad scale situation is most clearly understood by the current aloft as well as when viewed in their hemispheric setting. With this end in view, the remote sensing has been used to study the monsoon energetics over the Bay of Bengal by analysing the disturbed phases constituting cloud and monsoon depression fields during summer monsoon. The kinematic features, *e. g.*, vergence, vorticity, vertical velocities and pressure perturbations of a few selected disturbed phases have been studied in static and Lagrangian frame to evaluate a new optimum value of the disturbed phase maxima in terms of percentage cloud

* Department of Atmospheric Sciences, University of Wisconsin, Milwaukee, U.S.A.

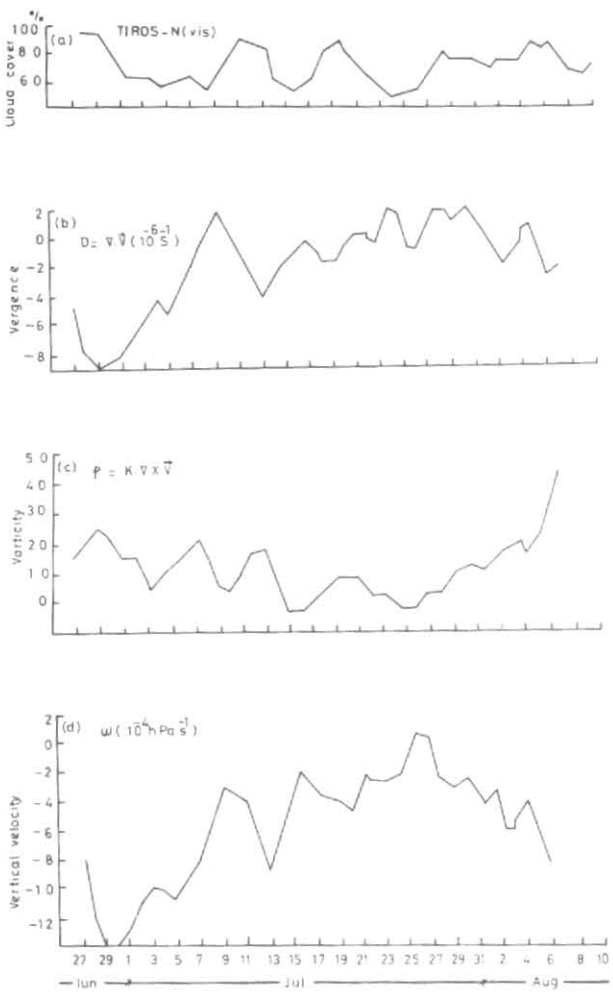

Figs. 1 (a-d). Plot over 10°×10° grid box of : (a) % cloud cover during 28 Jun-10 Aug 1979, (b) vergence. (c) vorticity, and (d) vertical velocity during 27 Jun-6 Aug 1979

coverage, lifetime and movement (direction and speed) of the depressions alongwith the optimum values of kinematic features over the Bay of Bengal, which may help to forecast the intensification of monsoon depressions in the Bay of Bengal before they affect Indian region.

Sikka and Gadgil (1980) examined the daily variation of Maximum Cloud Zones (MCZ) and the Inter-Tropical Convergence Zone (ITCZ) over Indian longitude during southwest (SW) monsoon by making use of NOAA satellite imageries of 1973-79. They found that the occurrence of MCZ was in the monsoon region north of 15°N. with a secondary MCZ in the equatorial region (0-10)°N. They also related its movement and life period to the monsoon activity.

Sikka (1980) studied southern hemispheric influence on the onset of SW monsoon of 1979 and observed that a transitory intensification of Mascarene

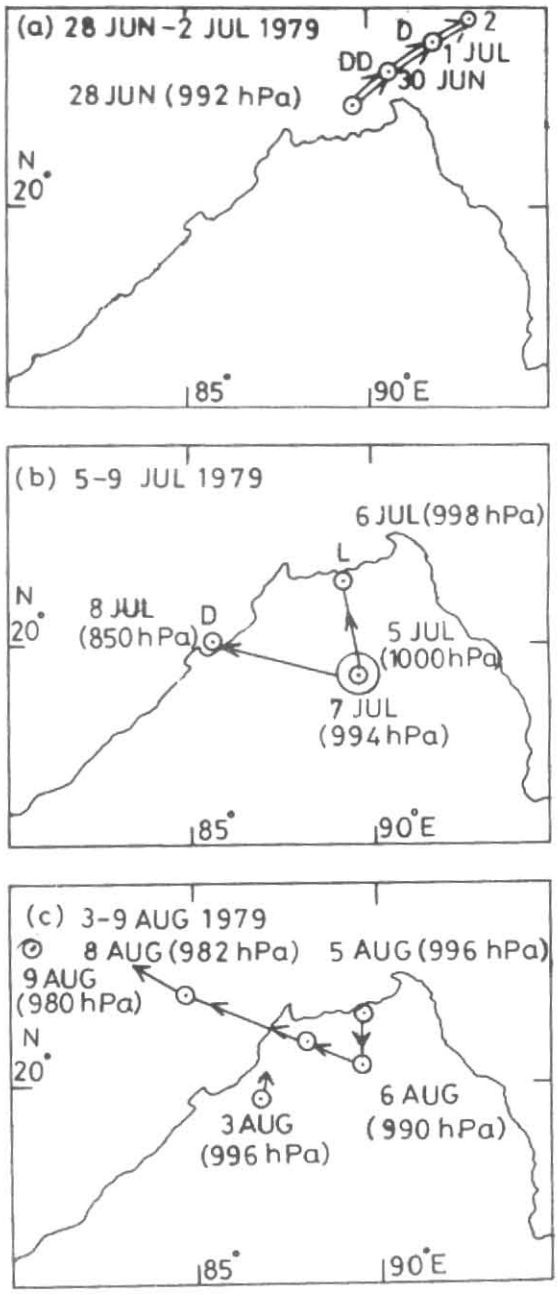

(b) 5-9 Jul, and (c) 3-9 Aug 1979

High, coupled with rapidly intensifying equatorial shear line provided for greatly increased crossed equatorial flow which set the stage for the monsoon incursion into India.

Sharma and Paliwal (1982) studied the monsoon structure of inland monsoon low, interpreting that the rainfall was more concentrated in the NW-NE sector during the day time.

Goswami *et al.* (1990) studied the characteristics of cloud clusters over southeast Asia (0-30°N and

TABLE 1

Mean SST over Bay of Bengal (10° × 10° grid box) during 28 June to 8 August 1979

Date (1979)	SST (°C)	Date (1979)	SST (°C)	Date (1979)	SST (°C)	Date (1979)	SST (°C)
28 Jun	28.0	9 Jul	—	20 Jul	—	31 Jul	—
29	29.0	10	—	21	26.0	1 Aug	29.3
30	28.6	11	—	22	28.0	2	—
1 Jul	29.0	12	—	23	28.0	3	—
2	29.0	13	—	24	—	4	—
3	29.0	14	—	25	29.0	5	29.0
4	—	15	26.0	26	—	6	28.0
5	—	16	30.0	27	—	7	27.0
6	28.0	17	28.0	28	—	8	27.0
7	27.0	18	—	29	28.0		
8	27.0	19	—	30	27.0		

70-120°E) during summer MONEX and found that the intense and large clusters (*i.e.*, lifetime averaged more than a day say 31 hrs) were related with monsoon depressions.

Goswami [1992(b)] studied the inter-hemispheric confluence zones during SW monsoon by making use of TIROS-N imageries of 1979 and found that Northern Hemispheric Confluence Zones (NHCZ) were greater in size, intensity and lifetime than Southern Hemispheric Confluence Zones (SHCZ) and the higher SSTs favoured their formation. Also, these confluence zones apparently governed the precipitation fields.

2. Data used

The TIROS-N imageries alongwith the FGGE levels IIb & level IIIb data obtained from University of Wisconsin, U.S.A. were used to study the disturbed phase characteristics, the daily precipitation in mm and the derived parameters of pressure, temperature and wind respectively. The grid point values of these parameters are separated by 1.875°/long. The drop wind sonde aircraft data was obtained from International Monex Management Centre (IMMC), New Delhi. The chronological weather summary of S-MONEX of Sikka and Grossman (1986) alongwith the Northern Hemispheric Analysis Centre (NHAC), New Delhi charts, provided the conventional weather information over the NH and SH regarding the day-to-day evolution of the large scale atmospheric circulation features during summer MONEX.

3. Analysis procedure

The Most Disturbed Phase (MDP) and Least Disturbed Phase (LDP) were identified by maxima and minima respectively in the percentage cloud coverage *vs.* time curve. The % cloud coverage for each month (June, July, August) was determined from the TIROS-N (IR day, IR night, visible) imageries by the method described by Goswami [1992(b)]. The disturbed phases selected for these studies appeared in the Bay of Bengal during 27 June-6 August 1979 [Fig. 6(a)].

The daily grid point values of u and v-components of wind velocities around the mass weighed centre of the cloud field within the 10° × 10° grid box (*i.e.*, 15-25°N × 85-95°E), were read from the FGGE level-IIIb data through UNIVAC computer system. The averaging was done to get the mean values at the centre of the 10° × 10° grid box. The mean divergence ($\bar{D}$) and the mean vorticity ($\bar{\xi}$) were computed over the specified area of Bay of Bengal (*i.e.*, 10° × 10°) grid box.

The vertical velocities ($\bar{w}$ hPa s^{-1}) were computed using the continuity equation, from the initialised divergence in the system. The computation was done for morning (0000 UTC) at 700 hPa and time series were plotted [Fig. 1 (d)]. Next, a change, if any, in a few selected thermodynamic and dynamic variables, *e.g.*, $\bar{D}$, $\bar{\xi}$, $\bar{w}$ were critically examined during the MDPs and LDPs.

The kinematic features of a typical disturbed phase in Lagrangian frame were studied by making use of MONEX-79 (FGGE and dropwind-sonde-aircraft) data and the nephanalysis results of TIROS-N imageries. A typical disturbed phase from 5 to 7 July 1979 with a small cloud peak (on 7 July) and large pressure perturbation was selected for examination of its kinematic features. The data profiles (u & v) have been drawn subsequently to identify the evolutionary features of the disturbed phase, *vis-a-vis* monsoon depression. The scheme is illustrated in Fig. 2(b) and u-v profiles are shown in Figs. 3 (a-f). The computation was done for forenoon hours.

The day-to-day pressure gradient at mean sea level was calculated between TRV-BMB (approximately along 75°E), JBP-NPT (approximately 80°E Long.) and AGT-PBL (approximately 93°E Long.) for the

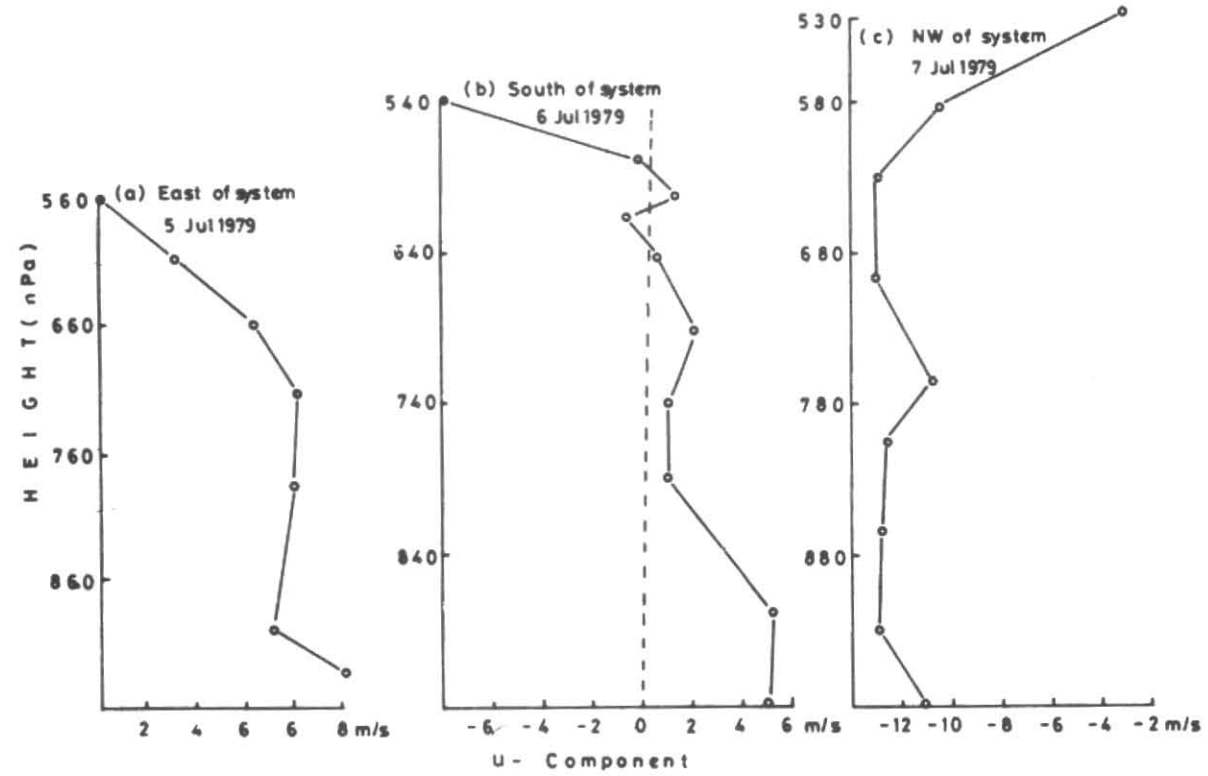

Figs. 3 (a-c). Study of depression in Lagrangian frame in u-component of: (a) 5 July 1979, east of system, (b) 6 July 1979, south of system, and (c) 7 July 1979, northwest of system

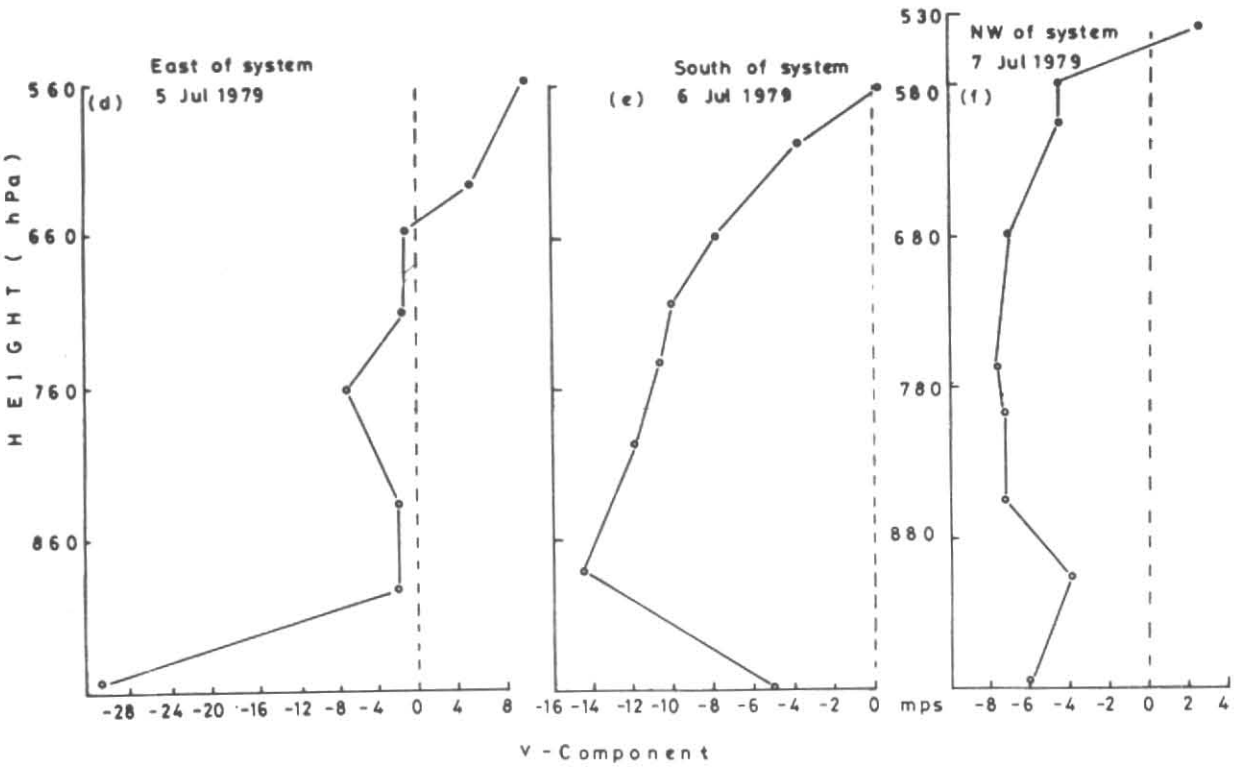

Figs. 3 (d-f). Study of depression of Lagrangian frame in v-component of: (d) 5 July 1979, east of system, (e) 6 July 1979, south of system, and (f) 7 July 1979, northwest of system

TABLE 2

Comparison of most disturbed phases of cloud fields and monsoon depressions over (10° × 10° grid box) during 27 June to 15 August 1979

Phase	Most disturbed phase				Life-time		Total life-time (days)
	Pre-disturbed phase	Peak day	Post-disturbed phase	Duration of MDP	Pre-disturbed (days)	Post-disturbed (days)	
I	28-30 Jun	1 Jul	2-4 Jul	28 Jun-4 Jul	5	3	7
II	5-6 Jul	7 Jul	8-9 Jul	5-9 Jul	5	2	5
III	2-5 Aug	6 Aug	7-9 Aug	2-9 Aug	7	3	8
IV	10-12 Aug	13 Aug	14-15 Aug	10-15 Aug	6	5	2
						Mean	6.5
Phase	Monsoon depression phase				Life-time		Total life-time (days)
	Forming stage	Matured stage	Dissipating stage	Total duration	Forming stage (days)	Dissipating stage (days)	
D_1	28-29 Jun	30 Jun	1-2 Jul	28 Jun-2 Jul	2	2	4
D_2	5-6 Jul	7 Jul	8-9 Jul	5-9 Jul	2	2	4
D_3	2-5 Aug	6 Aug	7-9 Aug	3-9 Aug	3	3	6
D_4	11-12 Aug	13 Aug	14-15 Aug	11-15 Aug	2	2	4
						Mean	4.5

month of June, July, August in the morning hours (0030 UTC). Time series were plotted [Figs. 4 (a-c)].

Next the Sea Surface Temperatures (SST's) over the 10°×10° grid box area were extracted from the IDWR (Table 1) to correlate with the kinematic parameters of selected disturbed phases of cloud and precipitation fields during 27 June-9 August 1979, in order to study the evolutionary features of monsoon depression.

From the conventional data, the depression phases were identified and the tracks of these D-phases have been pictorially represented in Figs. 2 (a-c).

Following Suchman *et al.* (1977) and the summer MONEX cloud cluster studies of Goswami *et al.* (1990), the two plausible models of monsoon depression have been postulated in terms of CCT and GCT.

TRV — Thiruvananthapuram, BMB — Bombay,
JBP — Jabalpur, NPT — Nagapattinam,
AGT — Agartala, PBL — Port Blair.

4. Results and discussion

The comparison of depression phases (D_1-D_3) and corresponding MDPs (I-III), during the period 27 June-6 August 1979 revealed that the lifetime of MDPs is greater than the depression phase corresponding to the mean values of 6.5 and 4.5 days respectively (Table 2). The finer analysis of these two phases revealed that the most disturbed phase constitutes the pre-disturbed and post-disturbed phase on its either side of the maxima [Fig. 1 (a)] and the depression phase is an admixture of known three stages, *viz.*, forming, mature and the dissipating stage (Table 2). Further, these sub-phases and sub-stages showed a definite correlation with each other, *i.e.*, the pre-disturbed and post-disturbed phases correspond to the formative and dissipating stage while the maxima (*i.e.*, cloud peak) refers to the mature stage of the monsoon depression. The computed values of lifetime indicated the longer span of pre-disturbed phases (3.75 days) than the post-disturbed phases (2.5 days), clearly revealing the fact that the formation of the monsoon depression is much slower than that of its dissipation and the same is well related to the cloud maxima with a considerable lag of 2 days' lifetime. Therefore, it is evident that from the satellite pictures one can reasonably forecast at least in two days advance, the formation and dissipation of a monsoon depression by determining the day of maxima in the most disturbed phases in terms of % cloud

coverage. The above noticed fact that the formation stage of a monsoon depression is of longer duration than that of its dissipation, may well be explained with the known morphological nature of monsoon depression (Godbole 1977) as well as by the deep convective mass transports by giant cumulus clouds, which form the major constituent of the formative and mature stage of a monsoon depression. Riehl and Malkus (1958) had shown that the upward transport of mass and energy is accomplished by giant cumulus clouds, *i.e.,* deep cumulus convection and motions of larger scales are inter-related. In the present investigation, the vertical mass transport has been explored by using the divergence field computed from the geostationary satellite winds (u & v-components) and vertical velocities to explain the monsoon energetics of Bay of Bengal *vis-a-vis* dynamical structure of monsoon depression during the disturbed phase in terms of satellite observed cloud fields during 27 June-6 August 1979.

The time series plot of vertical velocities ($\bar{w}$), [Fig. 1 (d)], for the period 27 June-6 August 1979 adumberates that the span of the rate of increase of vertical velocities (PQ & RS) are comparatively longer than the spans of decrease of vertical velocities (QR & ST) [Fig. 1 (d)]. This gives an important explanation of the above noticed fact that the forming stage of a monsoon depression is of greater duration than that of dissipating stage. Also, the computed mean divergence/convergence time series plot [Fig. 1 (b)], when studied with the satellite derived daily % cloud coverage [Fig. 1 (c)] for the period 27 June-6 August 1979, reveals the lesser values of convergence during the LDP, *i.e.,* the areas of minimum cloud coverage than that of MDP, *i.e.,* the areas of higher values of convergence and the maximum cloud coverage comprising of more convective type of clouding, resulting in more upward convective transport. This observation is in conformity with the studies of Reed and Ricker (1971) who had emphasised that the scale dependence of the inflow boundary layer mass and moisture convergence measured outside the cloudy part of a disturbance may be much less than an upward convective transport, if some of the mass and moisture converging on the disturbance of higher levels subsides and enters the boundary layer from above.

Indeed, this type of circulation has also been inferred during the present studies of a few monsoon depression phases (D_1-D_3), where subsidence was found outside the cloud canopy, commensurating with the lower values of convergence during the LDPs, *i.e.,* a time period of minimum or negligible satellite observed cloud coverage [Figs. 1 (a & b)]. This observation is in conformity with the studies made by Smith *et al.* (1975).

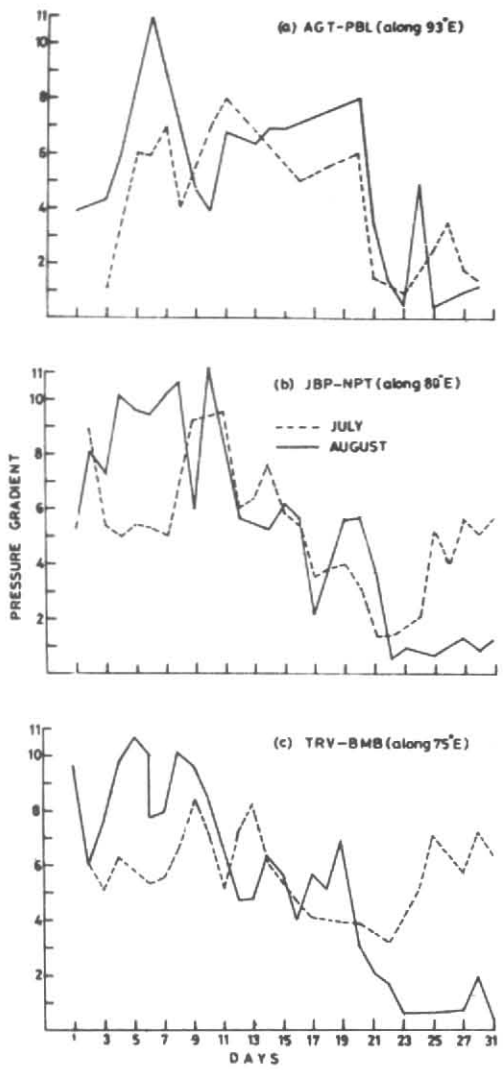

Figs. 4 (a-c). Pressure gradient between : (a) PBL & AGT, (b) JBP & NPT, and (c) TRV & BMB during July-August 1979 at 0300 UTC

From above discussions, one can summarise that the most disturbed phase in terms of cloud field of convective type is a precursor for the formation of monsoon depression. In other words, there has to be Conditional Instability of Second Kind (CISK) followed by instability which would give rise to monsoon depression (Saha and Shukla 1981). Further, the computation of periodicity of cloud fields and depression fields, revealed the greater number of cloud peaks than those of depression fields, inferring that it is not necessary for every MDP to match with the D-phase, but the reverse is true.

Table 3 represents the Surface Pressure Gradient (SPG) at 0300 UTC, between the two stations, selected in such a manner from east to west, that they fall approximately at the same latitude and along the same longitude, *viz.,* 93°E (PBL-AGT), 80°E (NPT-JBP) and

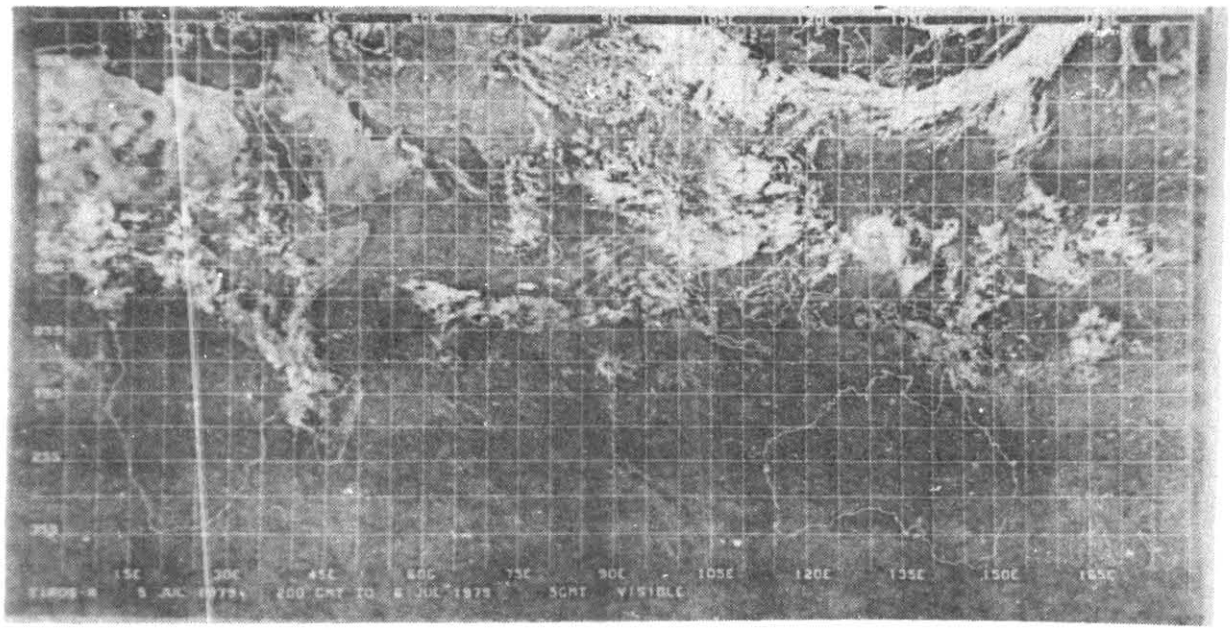

Fig. 5 (a). TIROS-N (VIS) 5 July 1979

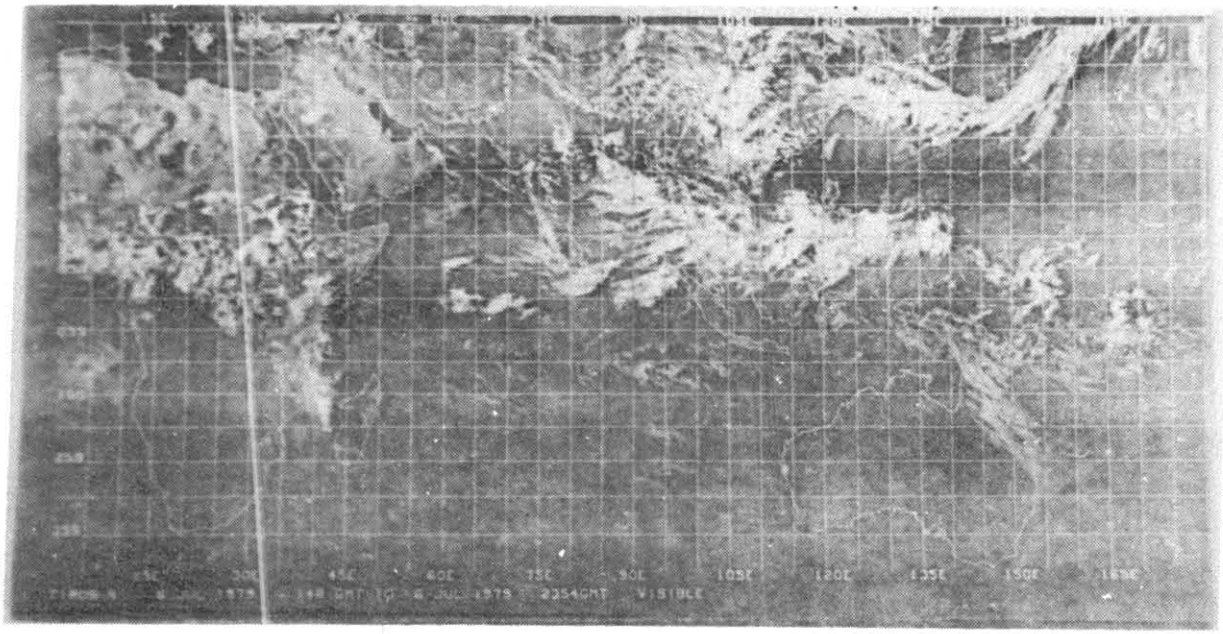

Fig. 5 (b). TIROS-N (VIS) 6 July 1979

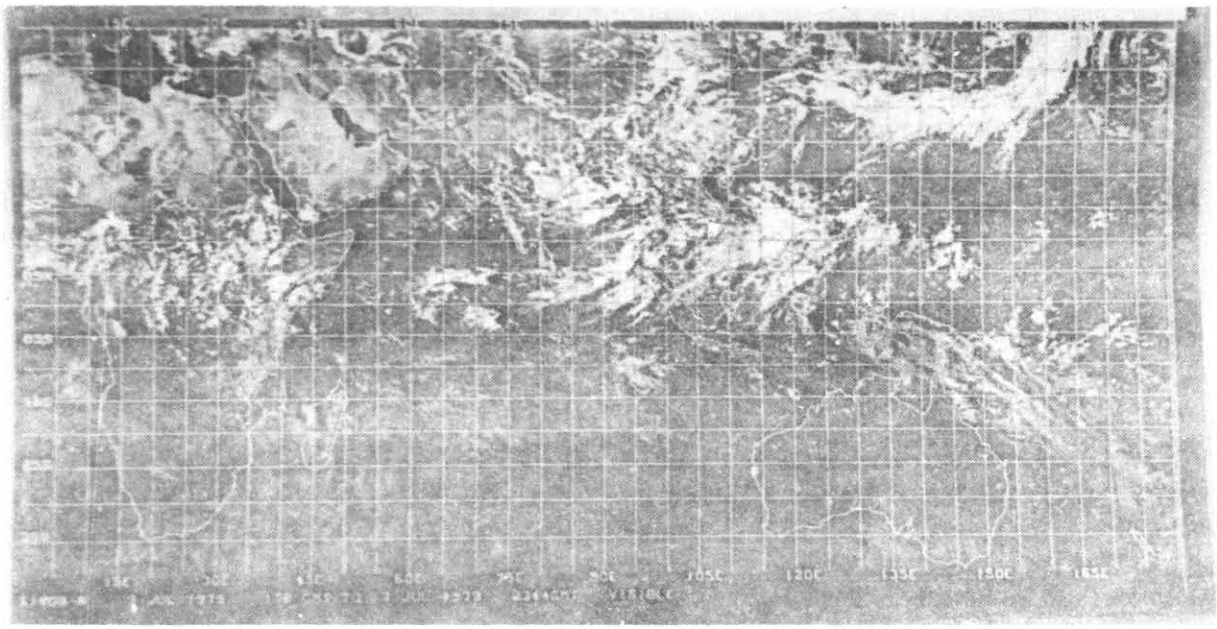

Fig. 5 (c). TIROS-N (VIS) 7 July 1979

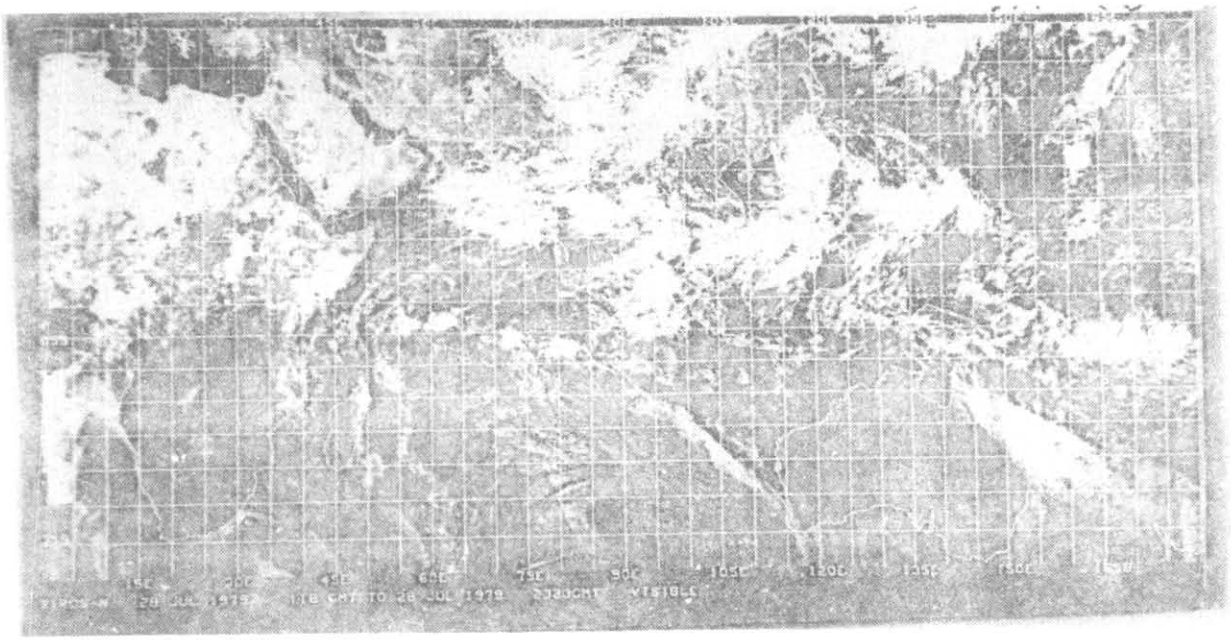

Fig. 5 (d). TIROS-N (VIS) 28 July 1979

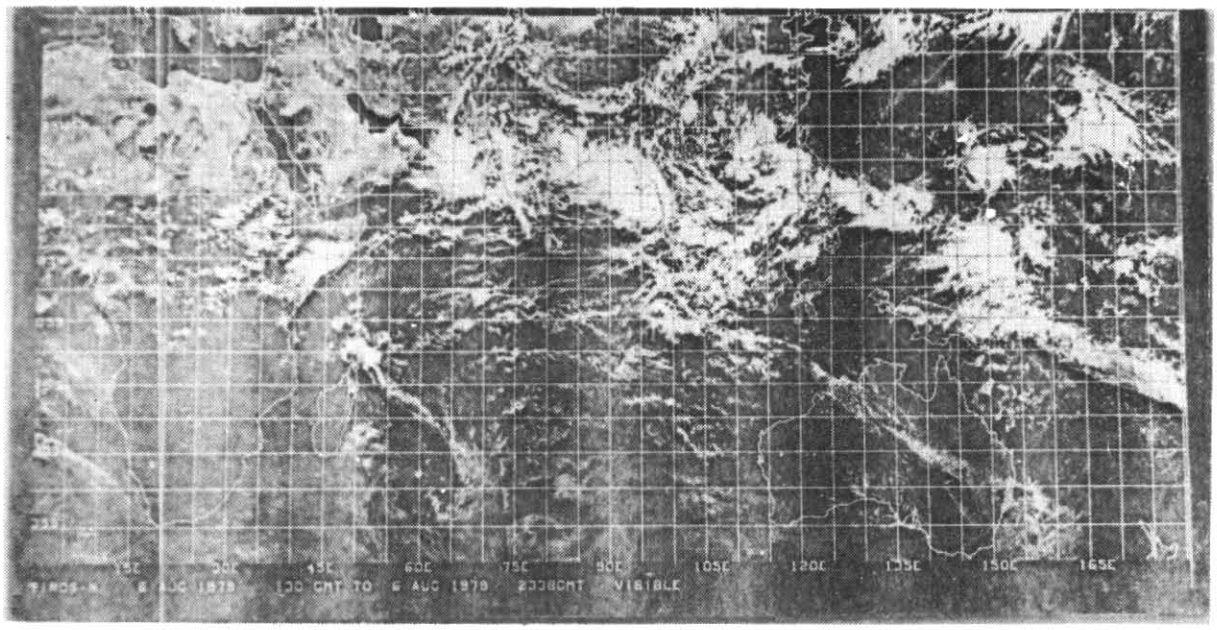

Fig. 5 (e). TIROS-N (VIS) 6 August 1979

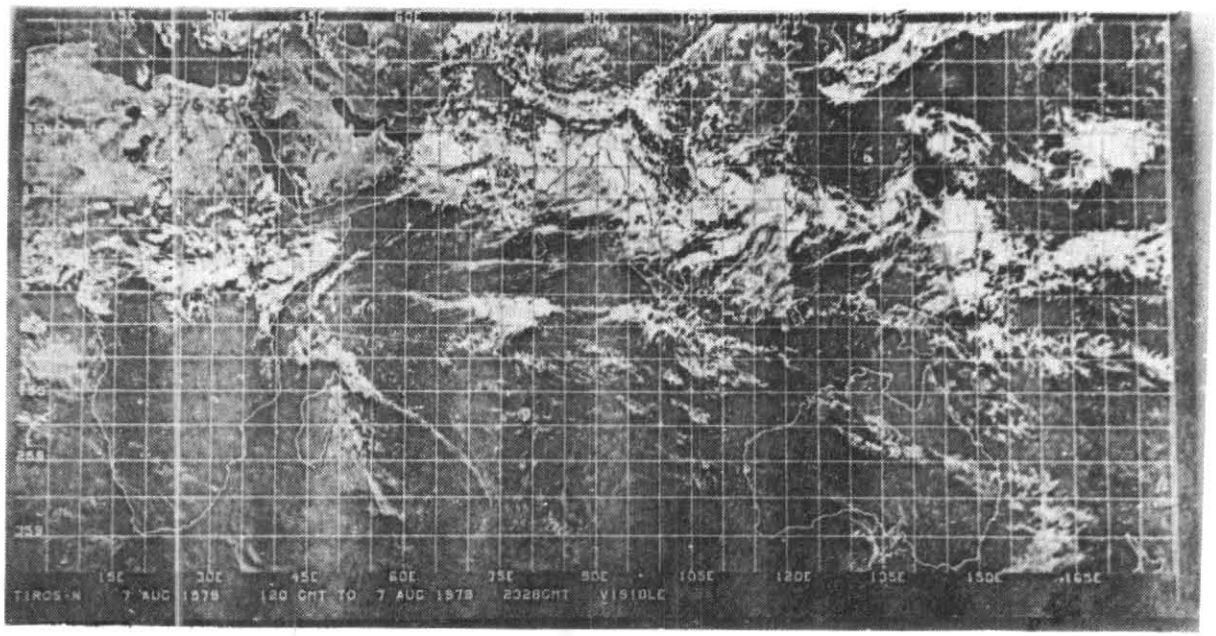

Fig. 5 (f). TIROS-N (VIS) 7 August 1979

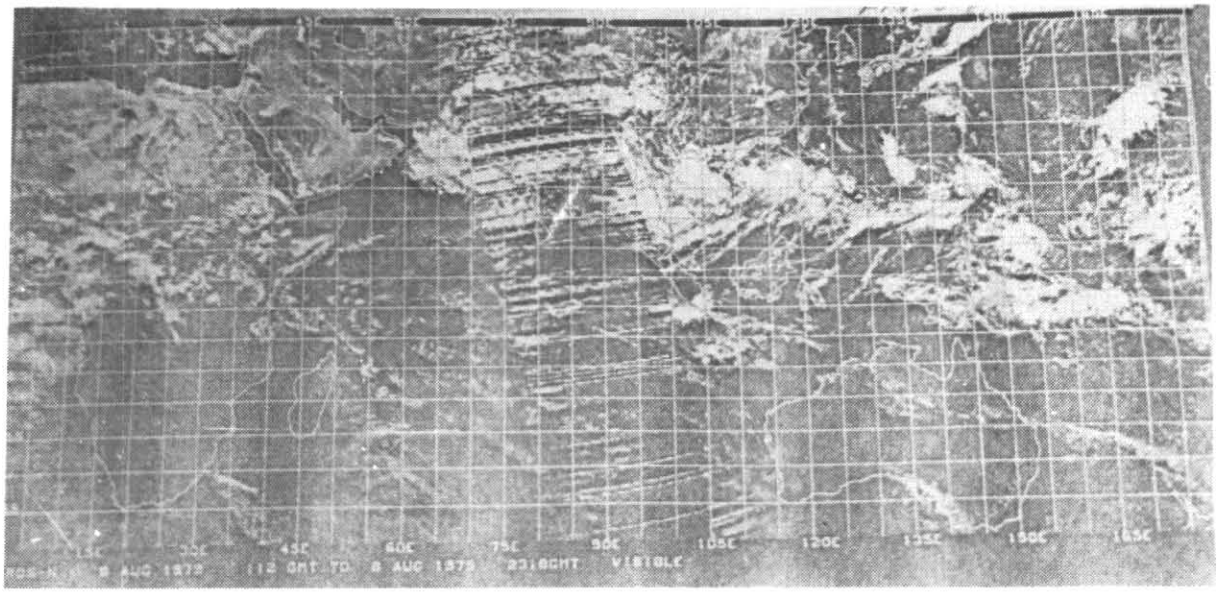

Fig. 5 (g). TIROS-N (VIS) 8 August 1979

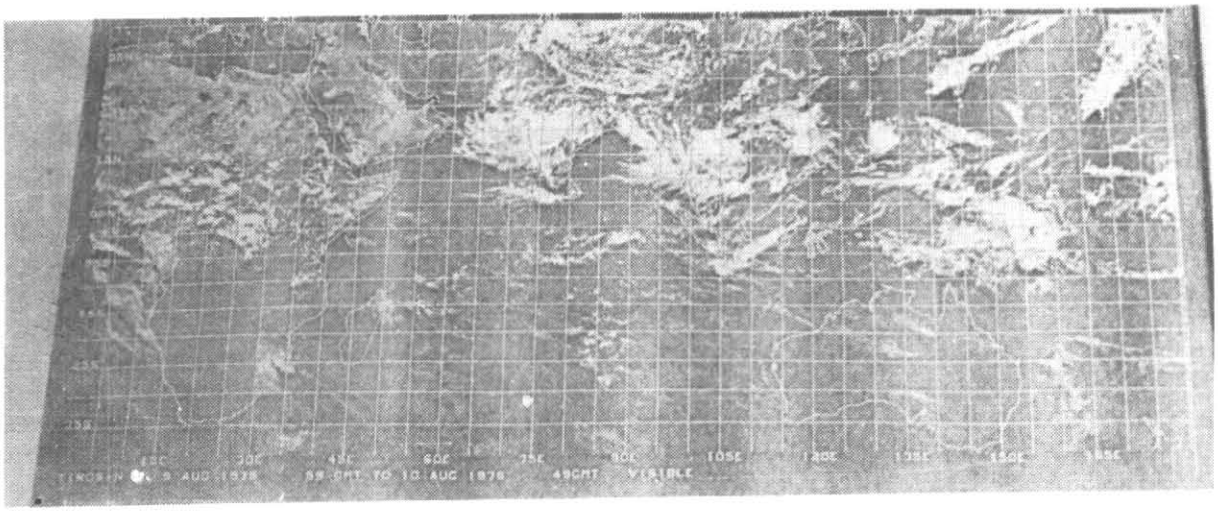

Fig. 5 (h). TIROS-N (VIS) 9 August 1979

TABLE 3

Longitudinal changes in Surface Pressure Gradient (SPG) during 28 June to 15 August 1979 at 0300 UTC

Month	Phase	Duration of phase	SPG along 93°E Port Blair-Agartala		SPG along 80°E Jabalpur-Nagapattinam		SPG along 75°E Bombay-Thiruvananthapuram	
			Day of maxima	Value of SPG at maxima (hPa)	Day of maxima	Value of SPG at maxima (hPa)	Day of maxima	Value of SPG at maxima (hPa)
Jul 1979	I	4-9 Jul	7 Jul	7	2 Jul	8.5	2 Jul 4 Jul	6.3 6.4
	II	10-17 Jul	13 Jul	7.6	12 Jul 14 Jul	9.2 7.6	10 Jul 14 Jul	8.2 7.7
	III	17-21 Jul	19 Jul	5.6	20 Jul	4.2	21 Jul	7.1
	Mean			6.7		7.5		7.0
Aug 1979	IV	4-9 Aug	6 Aug	10.7	2 Aug 4 Aug	7.6 10.2	1 Aug 5 Aug 9 Aug	9.5 10.4 9.8
	V	11-15 Aug	12 Aug	6.6	8 Aug 14 Aug	10.2 10.7	15 Aug	6.6
	Mean			8.5		9.6		9.0

75°E (TRV-BMB). The time series plots [Figs. 4 (a-c)] reveal that :

(a) *Along 93°E* — There are mainly three SPG maxima, *viz.*, 7, 13 and 19 July corresponding with MDPs 4-9 July, 14-17 July and 17-21 July respectively [Figs. 4 (a) & 1 (a)]. When compared with depression phase, it is observed that the pressure gradient is of the order of 6-7 hPa and more during the depression phase. Also, higher values of pressure gradient corresponded with the minimum pressure field in the 10° × 10° grid box area, conforming the most favourable orography, for the formation of intense cloud clusters, finally resulting into the well developed monsoon depressions (Goswami *et al.* 1990).

(b) *Along 80°E* — The principal SPG maxima are three in July (*i.e.*, 2, 12 and 17) and four in August (*i.e.*, 2, 4, 8 and 14) (Figs. 4-6). Although, the mean maximum values are greater in August (9 hPa or so) than that of July (*i.e.*, 7 hPa or so) but do not show any definite correlation between the MDPs or depression fields, inferring the less favourable longitudes for monsoon depression formation. This can be attributed to the dominance of smaller, less intense and short lived cloud clusters (Goswami *et al.* 1990), lesser density of NHCZ [Goswami 1992 (b)] and the lower SSTs (Table 1).

(c) *Along 75°E* — No definite relationship could be observed among cloud, precipitation and depression fields. However, SPG maxima on 2 July and 5 August did show relationship with cloud fields (MDPs) and depression fields (Ds). The higher values of 6-7 hPa and 9-10 hPa, in July and August respectively, were observed during the depression field inferring that when the monsoon depression either forms in the Arabian Sea or crosses into the Arabian Sea from the Bay of Bengal through the land mass of southern peninsula or rare occasions, then probably it again gets intensified due to land-ocean interactions, available moisture and wind convergence in the wake of southwesterly flow, during the southwest monsoon season. At this juncture, increased rainfall and clouding is observed over the coastal station of the southern peninsular region. Also, while studying the latitudinal variation of the satellite observed cloud fields, Goswami [1992(b)] observed increase clouding in the southern half of the 10° × 10° grid (*i.e.*, 15-20°N), and attributed to the high value of cyclogenesis favouring the intensification of monsoon depressions. In the present investigation it is seen that the LDPs (minimum cloud coverage) correspond to the non-depression phases except the anomaly of 28 July 1979, when more clouding in the northern half of 10° × 10°

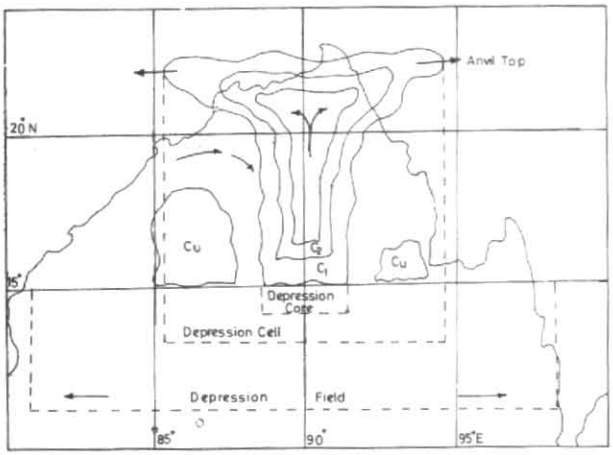

Fig. 6. Monsoon depression model

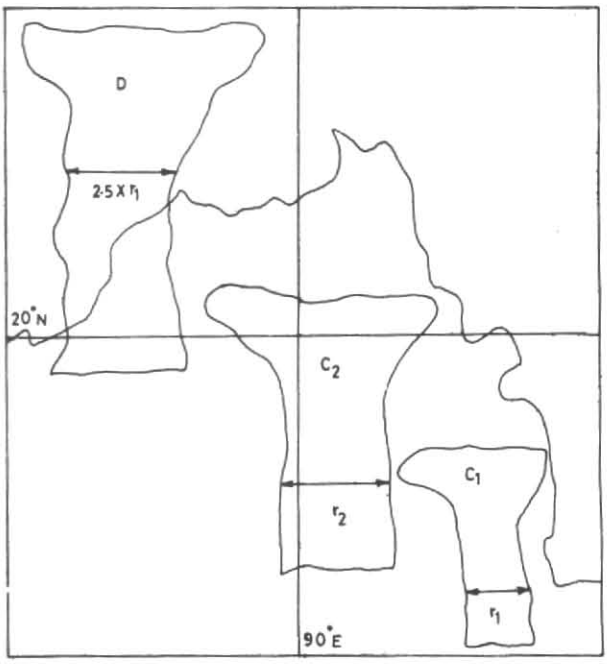

Fig. 7. Monsoon depression model

grid was observed than that of the southern half, due to persisting monsoon through at 20°N/85°E (Sikka & Grossman 1980).

An interesting thing was observed during the nephanalysis of available TIROS-N imageries, that the ITCZ lay between 5 & 15°N during the depression phases (Ds) *vis-a-vis* MDPs and shifted southward by 10°N (*i.e.,* between 5°N & 5°S) during the non-depression phases [Figs. 5 (a-h) TIROS-N-VR for 5, 6 7 & 28 July 1979 and 6, 7, 8 & 9 August 1979]. This gradual shift of ITCZ towards north from 0° to 15°N and subsequently persistence between 5 & 15°N, when compared with the history of monsoon during the complete period of summer monsoon (*i.e.,* 1 June to 31 August 1979), corresponds to the revival of summer monsoon depression respectively. This typical behaviour of ITCZ and corresponding MDPs and Ds may be explained by the tropical intrusion of cloud-bands of false cirrus, emanating from the convective cloud clusters of intense nature (*i.e.,* line of cumulonimbus clouds) existing in the ITCZ, by means of cross-equatorial flow causing the moisture incursion into the Indian sub-continent. The other plausible explanation may be incorporated on the basis of the earlier studies made by Goswami [1992 (a)] that there is some teleconnection of Southern Hemisphere features (*e.g.,* SHCZ, depression/cyclonic storms, equatorial troughs) with the identical features of northern hemisphere, governing the monsoon clouding/ monsoon activity over the region. This has been observed that the NHCZ were generally located to the north of ITCZ, keeping the SHCZ always south of it, *e.g.,* on 28 July 1979 [Fig. 5 (d)].

Kinematic features of a typical disturbed phase in the Lagrangian frame in association with the monsoon depression

For this, a typical disturbed phase (MDP) associated with well marked monsoon depression (D phase), occurred during 5-9 July 1979 was selected for the study of kinematic features in the Lagrangian frame. The *u* and *v* profiles were drawn for the period 5-7 July and following observations were recorded from the *u-v* plots [Figs. 3 (a-f) and Table 4].

The positive and negative values of *u*-component represent westerlies and easterlies winds while the northerlies and southerlies are represented by *v*- component respectively. It has been observed that low pressures are associated with strong westerlies to the east and weak westerlies to the south [Figs. 3 (a & b)]. The strong easterlies are seen upto the mid-tropospheric level in northern sector on 7th day of depression [Fig. 3 (c)]. As regards *v*-component, the strong southerlies (16-32 mps) were observed at lower levels with gradual reduction in speed on 5-6 July and a complete reversal of wind, *i.e.,* light, southerly (5 mps) at lower levels and gradual increase at higher level, took place on the depression day [*i.e.,* Fig. 3 (f)].

The results of vergence, vorticity and vertical velocities at 700 hPa for the period 27 June-6 August, comprising of the three monsoon depressions (D_1-D_3) for 0000 UTC are shown in Figs. 1 (b-d) respectively. The results are summarised in Table 5. During the depression phases (D_1-D_3) the highest values of convergence

TABLE 4

Study of monsoon depression in the Lagrangian frame

Lat 19.4°N/Long 92.0°E (5 July 1979 at 0349 UTC)			Lat 19.6°N/Long 88.7°E (6 July 1979 at 0524 UTC)			Lat 21.0°N/Long 87.8°E (7 July 1979 at 0328 UTC)		
Pressure (hPa)	*u* (mps)	*v* (mps)	Pressure (hPa)	*u* (mps)	*v* (mps)	Pressure (hPa)	*u* (mps)	*v* (mps)
566	1.7	7.2	483	−7.7	−7.0	531	−0.8	1.5
588	0.1	6.1	508	−1.7	−0.9	543	−3.2	1.7
612	3.1	4.3	534	−0.5	−4.0	564	−7.3	−3.3
635	5.5	0.2	558	−0.6	−5.9	594	11.4	−5.3
661	7.5	2.9	581	−1.1	−5.9	616	15.5	−3.9
689	7.8	4.1	604	−0.3	−8.0	640	−14.8	−5.3
718	8.4	5.4	628	−0.5	−9.0	667	−15.0	−5.4
747	9.3	4.7	656	1.7	−10.7	694	−14.1	−7.1
777	8.6	3.0	685	2.2	−10.5	724	−13.1	−8.5
808	9.3	2.7	711	2.5	−10.7	754	−11.8	−10.6
838	7.9	2.7	737	1.0	−11.1	782	−11.4	−10.5
868	9.2	3.9	764	0.2	−11.9	809	−13.1	−8.7
899	9.2	4.3	792	1.2	−14.1	837	−13.2	−9.9
929	9.1	4.1	821	2.2	−15.3	866	−13.4	−8.1
960	18.2	32.9	850	4.1	15.4	897	−13.7	−5.9
			880	5.6	−15.4	927	−15.6	−4.4
			913	7.3	−15.4	956	−12.8	−4.3
			942	5.7	−14.3	985	−11.2	−6.1

positive vorticity and vertical velocity, *i.e.*, negative values of match to maxima were observed. Similar was the case during MDPs (cloud field), resulting in maximum precipitation. Correspondingly, the lower values of vergence, vorticity and vertical velocities were recorded during LDPs and the days of no precipitation. The higher the vertical velocities more was the vertical mass transport. These higher values were favourable for the evolution of high cyclogenesis area, *vis-a-vis* monsoon depression. The finer comparison of these three fields with the depression phase, revealed the gradual increase during formation, peak values at mature and the decreasing values during dissipating stage of the depression (Table 5).

Similarly, when compared with the actual precipitation in terms of monsoon activity, comparatively higher values were observed during active monsoon than that of break and weak monsoon days. The gradual increase corresponded with the revival of monsoon. The same was the case with pressure showing maximum fall on the depression days. During active monsoon, there was hardly any fluctuation in the day-to-day msl pressure except that the small scale perturbations in pressure are seen during MDPs (days of highest % cloud coverage).

With the seggregation of the above results the monsoon energetic diagram comprising of the optimum values of the disturbed phase lifetime, % cloud coverage and SST (°C) are given below:

(i) Depression phase (D)
- Formation stage : 2-3 days
- Dissipating stage : 2-3 days
- Total life period : 4-5 days

(ii) Most disturbed phase (MDP)
- Pre-disturbed stage : 5.0 days
- Post-disturbed stage : 3.0 days
- Total life period : 6.5 days

(iii) Cloud coverage : > 80%
SST (Jul) : 28-29°C

The optimum values of the kinematic parameters have been shown in Table 6 and a plausible monsoon depression model for summer monsoon over the Indian regions has been devised (Figs. 6 & 7). The following two theories have been postulated to explain the devised monsoon depression model:

Cloud CCT of depression

The monsoon depression probably forms when an intense cloud cluster (consisting of large Cu & Cb) cells coalesce with another nearby intense cloud cluster cell and emerge into a bigger intense cloud cluster cell by the CISK mechanism. The process continues till the size of the bigger intense cloud cluster cell

TABLE 5

Kinematic parameters over 10° × 10° grid box during 27 June-6 August 1979

Name of phase	Mean vergence —ve value			Mean vorticity			Mean vertical velocity		
	Duration of phase	Day of maxima	Value at maxima ($\times 10^{-6}$ s^{-1})	Duration of phase	Day of maxima	Value at maxima ($\times 10^{-6}$ s^{-1})	Duration of phase	Day of maxima	Value at maxima ($\times 10^{-4}$ s^{-1})
MDP (cloud field)	27 Jun-3 Jul	30 Jun	9	27 Jun-1 Jul	30 Jun	25	27 Jun-3 Jul	30 Jun	17
	3-8 Jul	6 Jul	6	5-10 Jul	7 Jul	25	4-8 Jul	6 Jul	12
	10-15 Jul	12 Jul	4	10-14 Jul	12 Jul	15	9-15 Jul	13 Jul	9
	16-20 Jul	19 Jul	3	17-20 Jul	19 Jul	5	17-20 Jul	19 Jul	4
	25-28 Jul	27 Jul	3	25-27 Jul	26 Jul	5	24-27 Jul	26 Jul	3.5
	31 Jul-3 Aug	2 Aug	2	28-31 Jul	30 Jul	10	28-31 Jul	30 Jul	8
				31 Jul-3 Aug	2 Aug	20			
	4-6 Aug	6 Aug	3	4-6 Aug	6 Aug	40	4-6 Aug	2 Aug	15
Depression phase	D_1 28 Jun-2 Jul	30 Jun	9	D_1	30 Jun	25	D_1	30 Jun	14
	D_2 5-9 Jul	7 Jul	6	D_2	7 Jul	25	D_2	7 Jul	12
	D_3 3-9 Aug	6 Aug	3	D_3	6 Aug	40	D_3	6. Aug	15

TABLE 6

Optimum values of kinematic parameters

Disturbance phase	Month	SPG (hPa)			Mean at 700 hPa		
		75°E	80°E	93°E	Vertical vel ($\times 10^{-4}$ hPa s^{-1})	Vorticity ($\times 10^{-6}$ s^{-1})	Convergence ($\times 10^{-6}$ s^{-1})
D	Jun				14.0	25.0	9.0
	Jul				12.0	25.0	6.0
	Aug				15.0	40.0	3.0
MDP	Jun				17.0	25.0	9.0
	Jul	7.0	7.5	6.7	7.2	10.0	4.0
	Aug	9.0	9.6	8.5	15.0	30.0	2.5

reaches the size of the single large and intense cluster which corresponds to the monsoon depression by the process of coalesence of two or more intense cloud clusters. The size of such resulting intense large cloud cluster corresponds normally to that of D and with a lifetime of 31 hours or more (Goswami *et al.* 1990). Hence it can be shown that the monsoon depression cell (D) and the intense cloud clusters ($C_1, C_2, \ldots\ldots$) are inter-related by an equation

$$D = C_1 + C_2 + \ldots\ldots C_n.$$

If this theory is enhanced further then one can postulate a hypothesis of GDT for the monsoonal storms. Wherein, a monsoon depression grows into a very large and very intense monsoon depression, such as to match the intensity and size of cyclonic storm, through the sequential CISK mechanism, perhaps, inside the core of depression.

To authenticate these above theories (CCT & GDT), it would be worthwhile to compute kinematic features, *e.g.*, vergence, vorticity, and the mass transport, firstly, by counting the number of Intense Cloud Clusters (ICC) within a depression cell (D), followed by the computations of the vertical mass transport (M), within a single ICC, by using the method devised by Suchman *et al.* (1977).

They had found that the vertical mass transport (M) is related to divergence within the low level inflow layer and the high level outflow layer, and that this divergence can be inferred from measurement of cloud motions at the trade cumulus and cirrus level. The upward transport of mass in a deep/large Cu cloud (Mc) is related to the change in height and volume of cumulus, which can be inferred from geostationary

satellite imageries. They defined the mass transport through a surface as :

$$\bar{M} = \bar{\rho}\,\bar{A}\,\bar{w} \qquad (1)$$

where, the overbars denote an area average, ρ is the density, A area and w vertical velocity. Now if the estimates of M and Mc are available then the difference between M and Mc would result the transport M outside the deep convective clouds, as a residual. Assuming, incompressibility, through the equation of mass continuity, Eqn. (1) can be written as :

$$\bar{M} = -\frac{\Delta p h}{g}(\nabla . V_h) \qquad (2)$$

where, $\bar{M}$ now applies to the non-divergent/top or the bottom of layer of thickness Δp. g is gravity and $\nabla . V_h$ divergence averaged for the layer. $\bar{M}$ in this form is positive for transport out of the layer.

The depth of these layers may be inferred from soundings, geostationary satellite and radar measurements. Transports are assumed to be negligibly small at the top and bottom surface of the depression model. The winds in the inflow and outflow layers may be estimated from motions of trade cumulus and cirrus clouds by using Man-Computer-Interactive Data Access System (MCIDAS) (Suchman *et al.* 1977). Secondly, the assimilation of these results for individual ICC may be done with the number of ICCs present in the depression cell for quantitative estimation by means of satellite imageries, *i.e.*, remote sensing. It may be observed from the above monsoon depression model that there are three layers in vertical, *viz.*, inflow (*i.e.*, low tropospheric), outflow (*i.e.*, upper tropospheric) and the mid-tropospheric layer. This inflow layer at the lower level represents the ascending branch *vis-a-vis* updrafts. The outflow at the higher level refers to the descending branch *vis-a-vis* down drafts in an agglomerated, intense large cloud clusters, *i.e.*, depression, meeting the conditions of low-level convergence and high level divergence for its subsistence in conformity with the demand of mass continuity equation that the ascending branch of the vertical circulation be accompanied by a descending branch. This return flow (*i.e.*, outflow) may occur either within the depression cell/close to the depression cell, as an integral part of its circulation, or distant from it, as part of large circulation. This gives an insight into the horizontal structure of monsoon depression consisting of depression core (having two or more intense clusters, *i.e.*, field of intense convection), depression cell (*i.e.*, region of very intense convection), corresponding to area from approximate edge of cirrus shield and the depression field as an area much larger than that of the cluster field where monsoonal clouding is seen (Fig. 6). This depression field would be governed by the intensity of the depression, *i.e.*, the intense depression would have a more widespread field of influence.

The above CCT model holds good when ICCs are available in adequate number separated by the minimum distance in between. But, the cases have been observed when a single intense cluster has resulted into a depression when it moved into the favourable regions during the summer monsoons. Such cases can be explained by putting forward a new theory, *i.e.*, GCT.

GCT of monsoon depression (*Fig. 7*)

When an ICC (say C_2) of initial radius r_i grows either by CISK mechanism or due to peculiar orographic/thermodynamic features (*e.g.*, SSTs cyclogenesis) after having moved in favourable latitudes/longitudes from its place of origin, to the large radius of 2, 1/2 times more, then they match to the size of very intense large cloud cluster resulting into monsoon depression, *i.e.*, $D_2 = 2.5\ (r_i)$.

5. Conclusion

The present investigation shows that the quantitative interpretations of satellite imagery helps to infer the winds from the displacements of clouds, in satellite image sequences of three hourly interval. Also, by means of qualitative interpretation of TIROS-N (12 hourly interval) imageries one can trace the depressions by estimating the percentage cloud coverage and evolution of the cloud clusters, specially over data sparse regions of tropics. The study has brought out a plausible monsoon depression model supported by intense cloud CCT and GCT. The monsoon energetics diagram for Bay of Bengal during summer monsoon indicates a few optimum values of a few disturbed phases and may help in forecasting monsoon activity.

Acknowledgements

The senior author pays his homage with gratitudes to Professor D. N. Sikdar, Chairperson, Department of Atmospheric Sciences, University of Wisconsin, Milwaukee, U.S.A. for providing valuable suggestions, guidance, FGGE-data and computer facilities during his study leave (1982-84) from the Indian Air Force but for which it would not have been possible to complete this study. Special thanks are extended to Professor Verner Suomi and Dr. D. W. Mertin, Space Science

and Engineering Centre (SSEC), University of Wisconsin, Madison for providing TIROS-N satellite imageries and encouragement. Thanks to Sgt A. K. Mandal for drawing the figures. Sgt. A. A. Quarishi and PS3. C.P.L. Balan for typing this manuscript with great care and efficiency.

References

Godbole, R. V., 1977, "The composite structure of the monsoon depression", *Tellus*, **29**, 25-39.

Goswami, V. K., Martin, D. W. and Sikdar, D. N., 1990, "A satellite study of cloud clusters over southeast Asia during SMONEX-79", *Mausam*, **41**, 2, 177-182.

Goswami, V. K., 1992 (a), The quantitative application of remote sensing to study the tele-connection of southern hemispheric and northern hemispheric features of precipitation over southeast Asia. Abstract. TROPMET-92. National Symposium on Advances in Tropical Meteorology. India, p. 143.

Goswami, V. K., 1992 (b), Satellite observed cloud fields & inter hemispheric confluence zones during summer monsoon, unpublished—sent for National Symposium on Tropical Meteorology. TROPMET-93.

Reed, R. J. and Ricker, H. H., 1971, "Structure and properties of synoptic scale wave disturbances in the equatorial western Pacific", *J. Atmos. Sci.*, **28**, 1117-1133.

Riehl, H. and Malkus, J. N., 1958, "On the heat balance in the equatorial trough zone", *Geophysica*, **6**, 503-538.

Saha, K. and Shukla, J., 1981, Further evidence of westward propogation disturbances with monsoon depression during SMONEX-79, FGGE Report, **9**, 24-31.

Sharma, P. K. and Paliwal, R. K., 1982, "Mean structure of inland monsoon low", *Mausam*, **33**, 3, 333-342.

Sikka, D. R., 1980, Southern hemispheric influence and the onset of southwest monsoon of 1979, FGGE-GARP, **9**, Part 15, p. 23.

Sikka, D. R. and Gadgil, S., 1980, "On the maximum cloud zone and the ITCZ over the Indian longitudes during the southwest monsoon", *Mon. Weath. Rev.*, **108**, 1840-1853.

Sikka, D. R. and Grossman, 1980, A chronological weather summary for summer MONEX.

Suchman, D., Martin, D. W. and Sikdar, D. N., 1977, "Deep convective mass transports: An estimate from a geostationary satellite", *Mon. Weath. Rev.*, **105**, 943-955.

Smith, C. L., Zipser, E. J., Daggupaty, S. M. and Sapp, L. 1975, An experiment in tropical mesoscale analysis: Part-I, *Mon. Weath. Rev.*, **103**, 878-892.